Surface film formation on Mg electrode containing magnesium polysulfides in TFSI-based electrolytes

M. Victoria Bracamonte[1,2,=], Alen Vizintin[3,=], Gregor Kapun[3], Fernando Cometto[4], Jan Bitenc[3], Anna Randon-Vitanova[5], Miran Gaberščček[3,6], Robert Dominko[3,6,7,*]

[1]Instituto Enrique Gaviola (IFEG), CCT Córdoba-CONICET, 5000 Córdoba, Argentina.

[2]Facultad de Matemática, Astronomía y Física, Universidad Nacional de Córdoba (UNC), Av. Medina Allende s/n, Ciudad Universitaria, 5000 Córdoba, Argentina.

[3]National Institute of Chemistry, Hajdrihova 19, SI-1000, Ljubljana, Slovenia

[4]Departamento de Fisicoquímica, Instituto de Investigaciones en Fisicoquímica de Cordoba, INFIQC-CONICET, Facultad de Ciencias Químicas, Universidad Nacional de Córdoba, Ciudad Universitaria, X5000HUA Córdoba, Argentina

[5] Honda R&D Europe GmbH, Carl-Legien Strasse 30, 63703 Offenbach, Germany

[6]University of Ljubljana, Faculty of Chemistry and Chemical Technology, Večna pot 113, SI-1001, Ljubljana, Slovenia

[7]ALISTORE - European Research Institute, 33 rue Saint-Leu, Amiens 80039 Cedex, France

[=] These authors contributed equally to this work

*Corresponding author: Robert Dominko, email: robert.dominko@ki.si

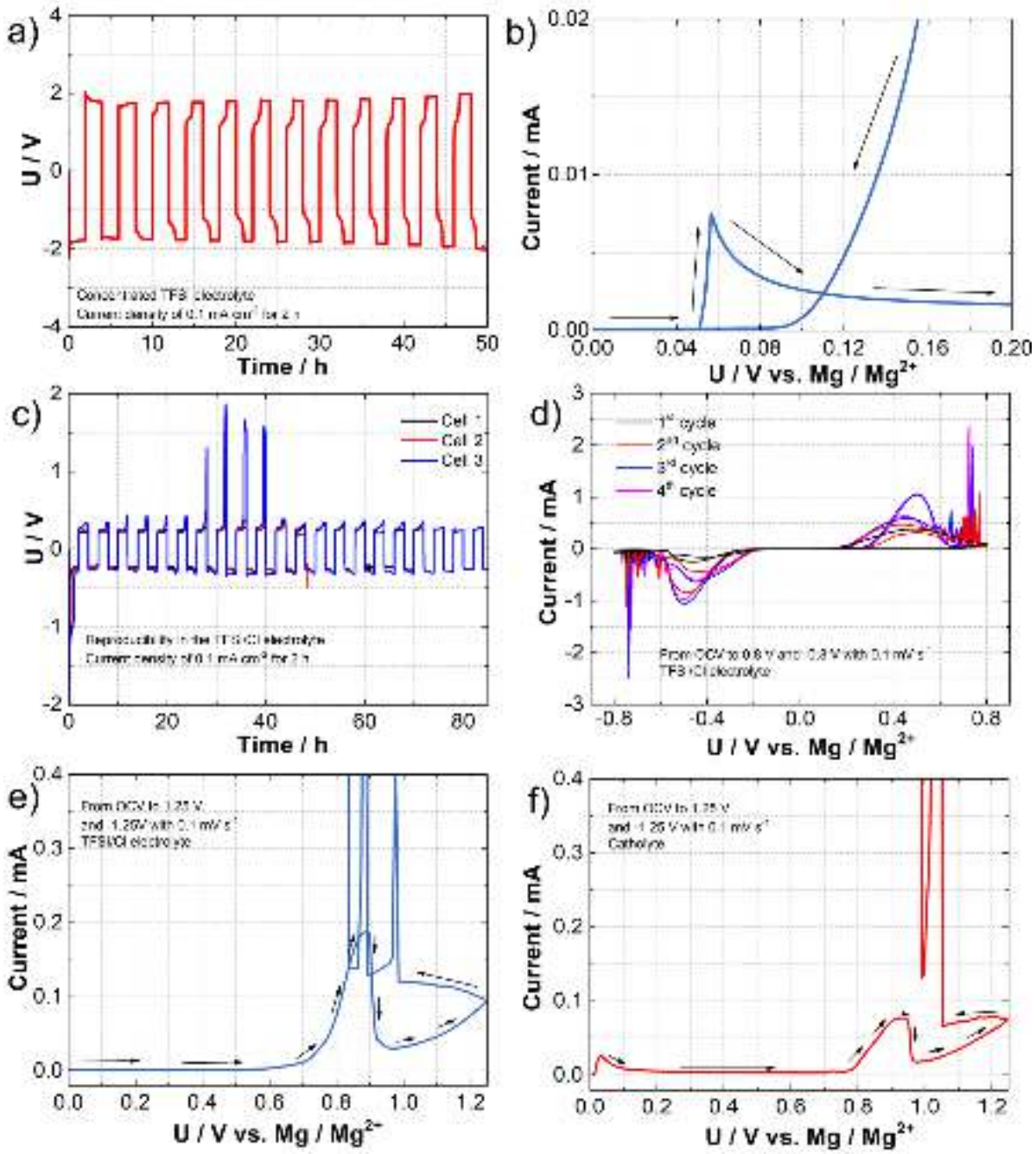

Figure S1. a) *Stripping/deposition profiles with a current density of 0.1 mA cm^{-2} and 2 h as cut-off of symmetrical Mg||Mg cells in concentrated TFSI electrolyte;* ***b)*** *CV magnification of Mg||Mg cell in TFSI/Cl electrolyte with a sweep rate of 0. 1 mV s^{-1} in the voltage range from 0.8 to –0.8 V;* ***c)*** *stripping/deposition profiles with a current density of 0.1 mA cm^{-2} and 2 h as cut-off of 3 symmetrical Mg||Mg cells in TFSI/Cl electrolyte;* ***d)*** *CV for symmetrical Mg||Mg cells in TFSI/Cl electrolyte; and CV with the potential cut-off was increased to 1.25 V for symmetrical Mg||Mg cells in* ***e)*** *TFSI/Cl electrolyte and* ***f)*** *catholyte*

General interfacial admittance for two adsorbed intermediates and code for EIS simulation

Derivation of general interfacial impedance involving adsorbed electrochemically active species follows the well-established procedures extensively used by Keddam *et. al.* on active-passive transition of iron[1–3] as well as our previous paper on the impedance response of copper in ammonia solutions.[4]

As shown in the Results and Discussion section, we here generally assume the following electrochemical and chemical reactions:

$$\mathrm{Mg} \underset{k_2}{\overset{k_1}{\rightleftarrows}} \mathrm{Mg}^{+}_{ads} + \mathrm{e}^{-} \qquad \text{(S1)}$$

$$\mathrm{Mg}^{+}_{ads} \underset{k_4}{\overset{k_3}{\rightleftarrows}} \mathrm{Mg}^{2+} + \mathrm{e}^{-} \qquad \text{(S2)}$$

$$\mathrm{Mg}^{+}_{ads} + \mathrm{A}^{-} \underset{K_6}{\overset{K_5}{\rightleftarrows}} \mathrm{MgA}_{ads} \qquad \text{(S3)}$$

$$\mathrm{MgA}_{ads} \underset{k_8}{\overset{k_7}{\rightleftarrows}} \mathrm{Mg}^{2+} + \mathrm{e}^{-} + \mathrm{A}^{-} \qquad \text{(S4)}$$

where k_i is a potential dependent rate constant, $k_i = k_{0,i} \exp\left(\frac{z\alpha_i F}{RT}\right) = k_{0,i} \exp(b_i E)$ whereisK_i are potential independent rate constants. $k_{0,i}$ is the rate at $E = 0$ determined with respect to a selected reference potential, z is the number of electrons exchanged in the step, α_i is the transfer coefficient, F is the Faraday's constant, R is the gas constant and T is temperature.

As we can see from (S1-S4), we assume the existence of two adsorbed species on the surface of magnesium, Mg^{+}_{ads} and MgA_{ads} with surface coverages θ_1 and θ_2, respectively. The possible nature of A is discussed in the main text.

The total current due to mechanism reactions (S1-S4) is:

$$I = F[(k_1 - k_4 - k_8)(1 - \theta_1 - \theta_2) + (k_3 - k_2)\theta_1 + k_7\theta_2] \qquad \text{(S5)}.$$

Mass balance relationships involving the adsorbed species are given by:

$$\beta_1 \frac{d\theta_1}{dt} = (k_1 + k_4)(1 - \theta_1 - \theta_2) - (k_3 + K_5 + k_2)\theta_1 + K_6\theta_2 \qquad \text{(S6a)},$$

$$\beta_2 \frac{d\theta_2}{dt} = K_5\theta_1 - (K_6 + k_7)\theta_2 + k_8(1 - \theta_1 - \theta_2) \qquad \text{(S6b)}.$$

At steady state conditions, the derivatives on the left are equal to zero and the surface concentrations become:

$$\bar{\theta}_1 = \frac{K_6(k_1+k_4+k_8)+k_7(k_1+k_4)}{K_5(k_1+k_4+k_7+k_8)+K_6(k_1+k_2+k_3+k_4+k_8)+k_7(k_1+k_2+k_3+k_4)+k_8(k_2+k_3)} \qquad \text{(S7a)},$$

$$\bar{\theta}_2 = \frac{K_5(k_1+k_4+k_8)+k_3k_8}{K_5(k_1+k_4+k_7+k_8)+K_6(k_1+k_2+k_3+k_4+k_8)+k_7(k_1+k_2+k_3+k_4)+k_8(k_2+k_3)} \quad \text{(S7b)}.$$

The steady state current then reads:

$$\bar{I} = F\frac{2k_1(k_3k_7+K_5k_7+k_3K_6)}{k_3(k_7+k_8)+K_5(k_1+k_4+k_7+k_8)+K_6(k_1+k_3+k_4+k_8)+k_7(k_1+k_4)} \quad \text{(S8)}.$$

The interfacial admittance is obtained by differentiation of Eq. (S5):

$$\frac{1}{F}\frac{\partial I}{\partial E} = (b_1k_1 + b_4k_4 + b_8k_8)(1-\theta_1-\theta_2) + (b_3k_3 + b_2k_2)\theta_1 + b_7k_7\theta_2 + (-k_1-k_2+k_4+k_3+k_8)\frac{\partial\theta_1}{\partial E} + (-k_1+k_4+k_7+k_8)\frac{\partial\theta_2}{\partial E} \quad \text{(S9)}.$$

The partial derivatives $\partial\theta_i/\partial E$ are obtained according to the following procedure. Differentiating the current, which depends on the potential and surface coverages, we obtain:

$$\delta I = \left(\frac{\partial I}{\partial E}\right)_{\theta 1,\theta 2}\delta E + \left(\frac{\partial I}{\partial \theta_1}\right)_{E,\theta 2}\delta\theta_1 + \left(\frac{\partial I}{\partial \theta_2}\right)_{E,\theta 1}\delta\theta_2 \quad \text{(S10)}.$$

Faradaic admittance of the interface is then defined as:

$$Y_F \equiv \frac{\partial I}{\partial E} = \left(\frac{\partial I}{\partial E}\right)_{\theta 1,\theta 2} + \left(\frac{\partial I}{\partial \theta_1}\right)_{E,\theta 2}\left(\frac{\partial\theta_1}{\partial E}\right) + \left(\frac{\partial I}{\partial \theta_2}\right)_{E,\theta 1}\left(\frac{\partial\theta_2}{\partial E}\right) \quad \text{(S11)}.$$

Too calculate explicitly Y_F, we need to know how θ_1 and θ_2 depend on E. These relations are usually found from the corresponding mass balance equations.[1,2] For the case of two species adsorbed in a form of a monolayer, these can be generally written as:

$$\beta_1\frac{d\theta_1}{dt} = f(E,\theta_1,\theta_2) \quad \text{(S12a)},$$

$$\beta_2\frac{d\theta_2}{dt} = g(E,\theta_1,\theta_2) \quad \text{(S12b)},$$

where β_1 and β_2 are the complete monolayer surface concentrations of both adsorbed species, respectively, while t is time.

Functional dependencies f and g in Eqs. (S12a,b) crucially determine the actual surface model. The present form already implicitly assumes that both coverages are correlated because both f and g contain dependence on both surface coverages, θ_1 and θ_2. This interdependence of both surface species somewhat complicates the further treatment. For an example, we are not aware of any equivalent circuit that has been developed for such a model. Nevertheless, a closed form solution for the admittance given by Eq. (S11) is still possible. Thus, after Fourier

transforming[1] and differentiating Eqs. (S12a,b), one can get the explicit forms for the two unknown derivatives in Eq. (S11):

$$\left(\frac{\partial\theta_1}{\partial E}\right)=\frac{\frac{df}{dE}\frac{dg}{d\theta_2}-\frac{df}{d\theta_2}\frac{dg}{dE}-j\omega\beta_2\frac{df}{dE}}{\frac{df}{d\theta_2}\frac{dg}{d\theta_1}-\frac{df}{d\theta_1}\frac{dg}{d\theta_2}+\omega^2\beta_1\beta_2+j\omega\left(\beta_2\frac{df}{d\theta_1}+\beta_1\frac{dg}{d\theta_2}\right)} \qquad \text{(S13a)},$$

$$\left(\frac{\partial\theta_2}{\partial E}\right)=\frac{\frac{dg}{dE}\frac{df}{d\theta_1}-\frac{df}{dE}\frac{dg}{d\theta_1}-j\omega\beta_1\frac{dg}{dE}}{\frac{df}{d\theta_2}\frac{dg}{d\theta_1}-\frac{df}{d\theta_1}\frac{dg}{d\theta_2}+\omega^2\beta_1\beta_2+j\omega\left(\beta_2\frac{df}{d\theta_1}+\beta_1\frac{dg}{d\theta_2}\right)} \qquad \text{(S13b)},$$

where $j = \sqrt{-1}$. Inserting Eqs. (S13a,b) into Eq. (S11) one readily calculates the faradaic admittance (the inverse of faradaic impedance) of the system. Usually, the final interfacial impedance takes into account the double layer capacitance, *Cdl*, which is empirically added in parallel to the faradaic impedance (here the typical value is around 1 μF).

Example of the code for simulation of graphs in Figure 3b together with the specific impedance output is given below.

Example of code (Python):

```
#Miran Gaberscek, August 2021
import numpy as np
import matplotlib.pyplot as plt
omega=6.28e-2
DiscrRe=[]
DiscrIm=[]
while omega<1e6:
    E=0
    E0=0
    Far=96500
    b1 = 19.5
```

[1] In order to avoid unnecessary complication, we do not introduce special notation for Fourier transformed quantities.

```
b2 = 19.5
b3 = 19.5
b4 = 19.5
b7 = 19.5
b8 = 19.5

k10= 1.6e-8 *2
k20= 1e-15
k30= 1.5e-11 /1.6
k40= 1e-13
k70= 1e-12
k80= 1e-15
K5= 4e-11
K6= 1e-11
beta1= 3e-8 *10
beta2= 7e-9 *10

k1=k10*np.exp(b1*(E-E0))
k2=k20*np.exp(-b2*(E-E0))
k3=k30*np.exp(b3*(E-E0))
k4=k40*np.exp(-b4*(E-E0))
k7=k70*np.exp(b7*(E-E0))
k8=k80*np.exp(-b8*(E-E0))

the1rav=(K6*(k1+k4+k8)+k7*(k1+k4))/(K5*(k1+k4+k7+k8)+K6*(k1+k2+k3+k4+k8)+k7*(
k1+k2+k3+k4)+k8*(k2+k3))
the2rav=(K5*(k1+k4+k8)+k3*k8)/(K5*(k1+k4+k7+k8)+K6*(k1+k2+k3+k4+k8)+k7*(k1+k2
+k3+k4)+k8*(k2+k3))
    OdvFPot=(b1*k1-b4*k4)*(1-the1rav-the2rav)-(b3*k3-b2*k2)*the1rav
    OdvFThe1=-k1-k2-k3-k4-K5
    OdvFThe2=-k1-k4+K6
    OdvGPot=-b7*k7*the2rav+b8*k8*(1-the1rav-the2rav)
    OdvGThe1=K5-k8
    OdvGThe2=-K6-k7-k8
```

```
    imen=OdvFThe2*OdvGThe1-
OdvFThe1*OdvGThe2+omega**2*beta1*beta2+1j*omega*(beta2*OdvFThe1+beta1*OdvG
The2)

    OdvThe1Pot=(OdvFPot*OdvGThe2-OdvFThe2*OdvGPot-
1j*omega*beta2*OdvFPot)/imen

    OdvThe2Pot=(OdvGPot*OdvFThe1-OdvFPot*OdvGThe1-
1j*omega*beta1*OdvGPot)/imen



    adm=(b1*k1+b4*k4+b8*k8)*(1-the1rav-
the2rav)+(b3*k3+b2*k2)*the1rav+b7*k7*the2rav+(-k1-k2+k4+k3+k8)*OdvThe1Pot+(-
k1+k4+k7+k8)*OdvThe2Pot

    imp1=1/(adm*Far)

    imp2=1/(1/imp1+1j*omega*1e-6)

    imp=1/(1/(120+imp2)+1j*omega*1.5e-6)

    DiscrRe.append(imp2.real)

    DiscrIm.append(-imp2.imag)

    omega=omega*1.1
#plotting

plt.plot(DiscrRe,DiscrIm,'-',mfc='none',linewidth=1)

plt.axes().set_aspect('equal')

plt.xlabel(r'$\mathrm{Re}(Z) \, /\, \mathrm { \Omega } $',fontsize=16)

plt.ylabel(r'-$\mathrm{Im}(Z) \,/\, \mathrm { \Omega } $',fontsize=16)

plt.tight_layout()

plt.show()
```

The output of the code:

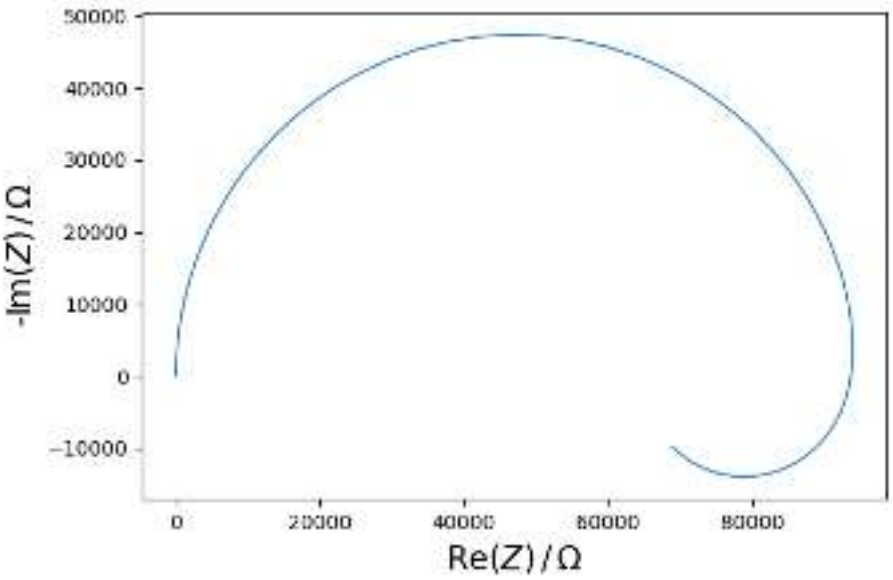

Figure S2: *Example of the simulated EIS spectra*

Table S1. *Typical values of kinetic parameters used in impedance simulations. Note that non-normalized values are given, i.e. the values that directly correspond to the non-normalized impedance units given in Figure 3. For normalization per unit surface area unit one needs to be taken into account the total electrode surface area of 4 cm^2 (2 cm^2 per each electrode in a symmetrical cell setup).*

Parameter [unit]	**Fig3a (magenta spectrum)**	**Fig3b (magenta spectrum)**
b_i [V^{-1}]	19.5	19.5
C_{DL} [F]	1×10^{-6}	1×10^{-6}
$k_{0,1}$ [mol s^{-1}]	1.4×10^{-7}	3.2×10^{-8}
$k_{0,2}$ [mol s^{-1}]	2.1×10^{-16}	1.0×10^{-15}
$k_{0,3}$ [mol s^{-1}]	1.8×10^{-13}	9.4×10^{-12}
$k_{0,4}$ [mol s^{-1}]	2.1×10^{-13}	1.0×10^{-13}
K_5 [mol s^{-1}]	N/A	4.0×10^{-11}
K_6 [mol s^{-1}]	N/A	1.0×10^{-11}
$k_{0,7}$ [mol s^{-1}]	N/A	1.0×10^{-12}
$k_{0,8}$ [mol s^{-1}]	N/A	1.0×10^{-15}
β_1 [mol]	1×10^{-8}	3.0×10^{-7}
β_2 [mol]	N/A	7.0×10^{-8}

ATR-IR spectroscopy at the magnesium electrode surface

We have performed the ATR-IR measurements inside the glovebox on a Bruker Alpha II equipped with a germanium ATR crystal with 128 scans and 4 cm^{-1} resolution from 4000 to 700 cm^{-1}. Figure S3 shows the used electrolyte ($Mg(TFSI)_2/MgCl_2$ in TEGDME:DOL), the electrolyte components ($Mg(TFSI)_2$, $MgCl_2$ and solvents) and the (non)cycled magnesium electrodes. The used $Mg(TFSI)_2/MgCl_2$ in TEGDME:DOL electrolyte has a complex IR spectra (figure S3a), which is mainly composed from $Mg(TFSI)_2$, at 1362 and 1325 cm^{-1} (SO_2 asymmetric and symmetric stretching vibration), TEGDME at around 1100 cm^{-1} (broad C–O and C–C stretching vibration), 850 cm^{-1} (CH_2 rocking vibration) and DOL contribution at 1059 cm^{-1} (C–O stretching vibration), 919 cm^{-1} (CH_2 rocking vibration). The $MgCl_2$ shows very low absorption vibrations at around 1600 cm^{-1}. Additionally, in the figure S3b, the non-cycled and cycled magnesium electrode is presented. The non-cycled magnesium electrode shows weak IR signals on the surface, presumably due to small presence of MgO. This is confirmed by SEM-EDX measurements (figure S4). On the other hand, the cycled magnesium electrode surface is different. At the cycled magnesium surface is possible to observed mainly the degradation products from the $Mg(TFSI)_2$ salt. The degradation $Mg(TFSI)_2$ products was further confirmed by the measured XPS, which give us more in deep information about the decomposition products.

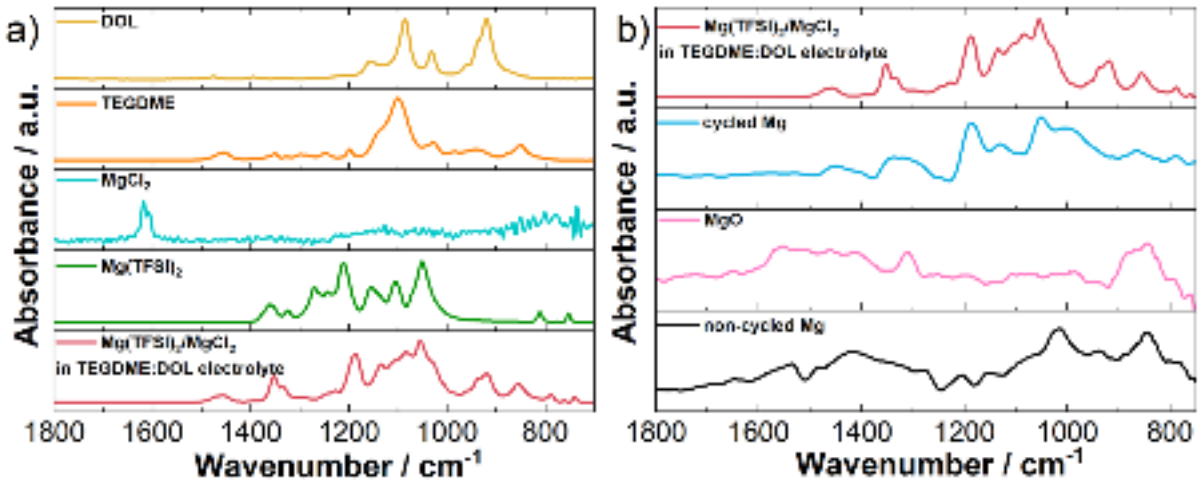

Figure S3: ***a)*** *ATR-IR spectra of the $Mg(TFSI)_2/MgCl_2$ in TEGDME:DOL electrolyte and its separate components and* ***b)*** *ATR-IR spectra of the (non)-cycled magnesium electrode surface.*

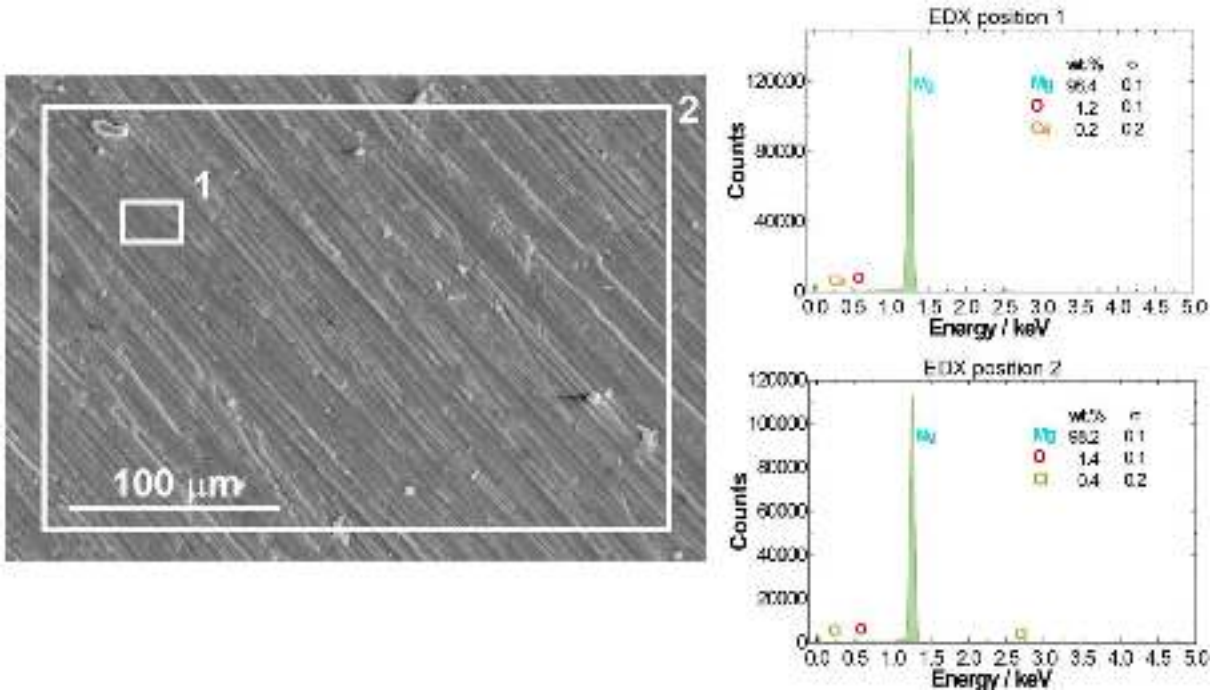

Figure S4: *EDX surface mapping for fresh Mg electrode*

SEM imaging of various Mg electrode surfaces and cross-section

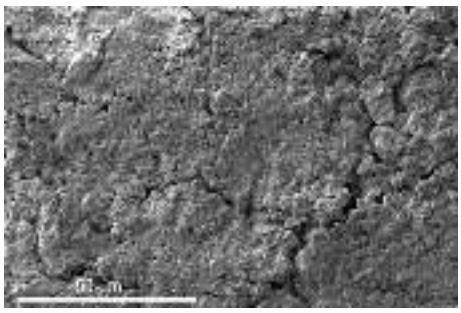

Figure S5. *SEM top-down micrographs of cycled magnesium electrode in concentrated TFSI electrolyte.*

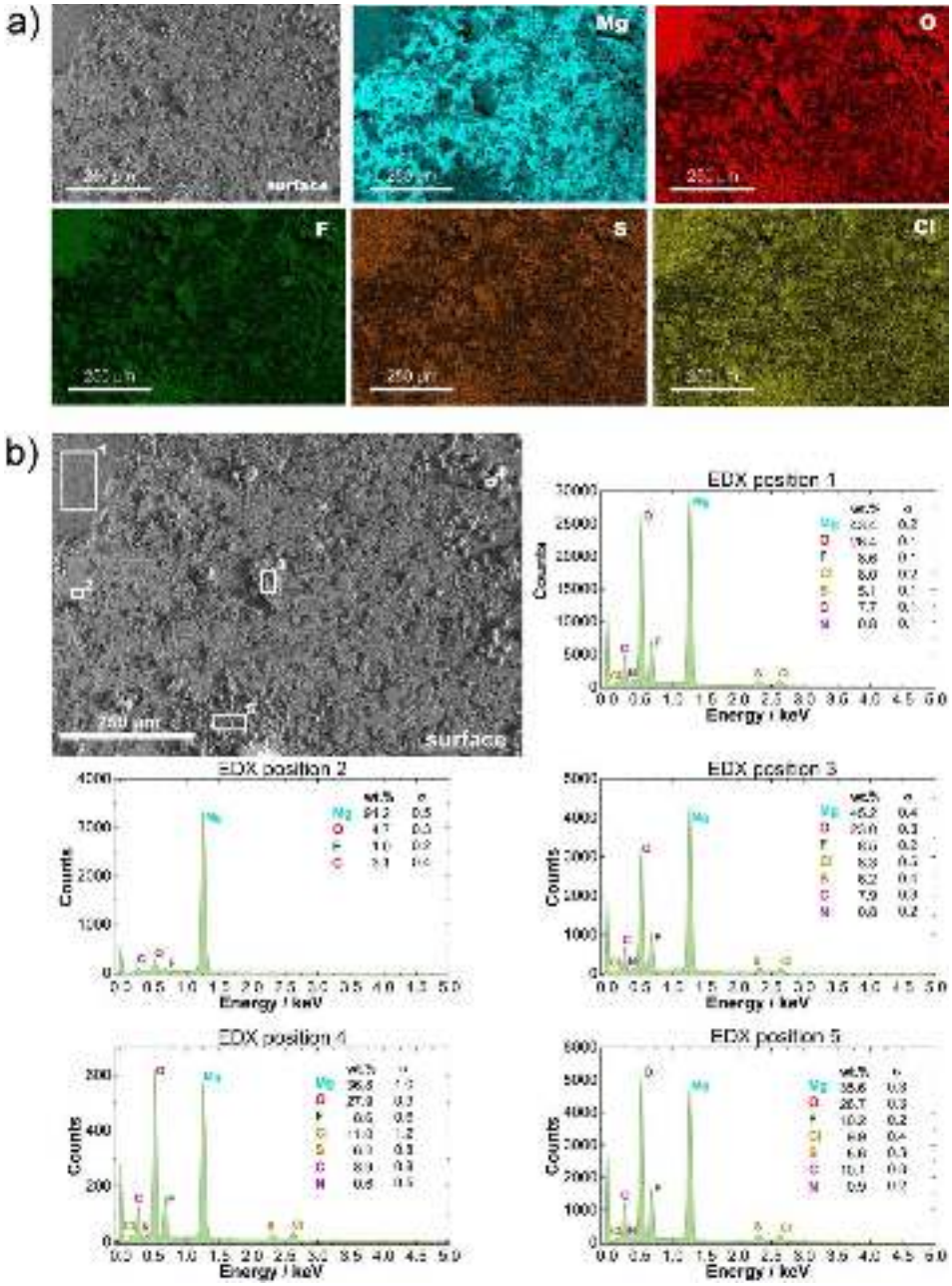

Figure S6. a)*.EDX surface mapping for cycled Mg electrode with TFSI/Cl electrolyte and* ***b)*** *quantitative EDX spectra of selected areas*

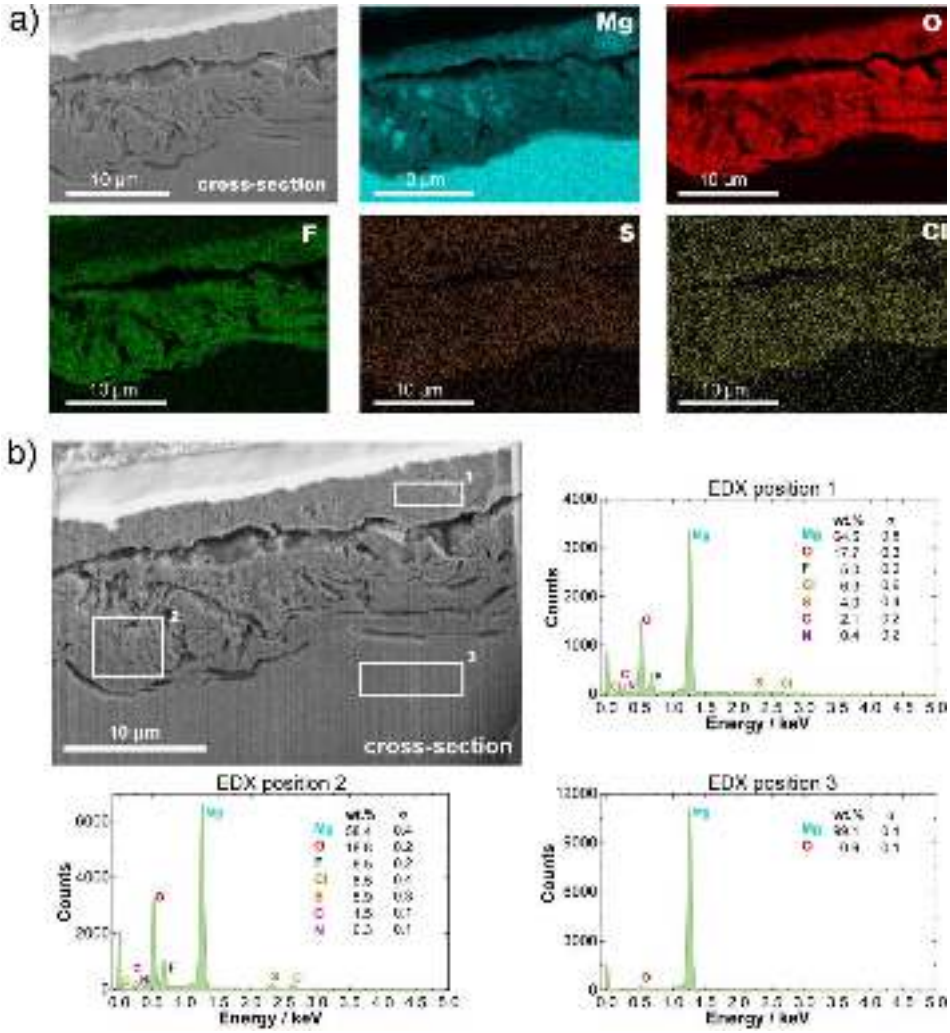

Figure S7. a)*.EDX cross-section mapping for cycled Mg electrode with TFSI/Cl electrolyte and* ***b)*** *quantitative EDX spectra of selected areas*

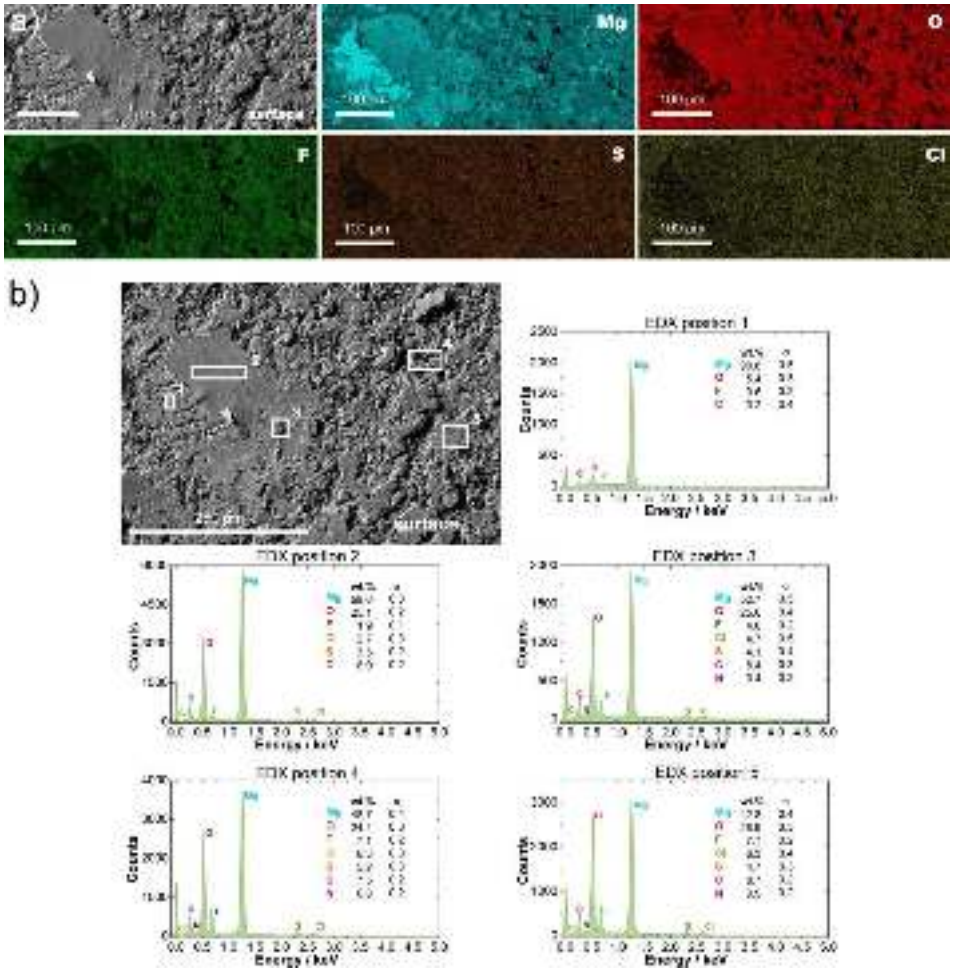

Figure S8. a)*.EDX surface mapping for cycled Mg electrode with catholyte and* ***b)*** *quantitative EDX spectra of selected areas*

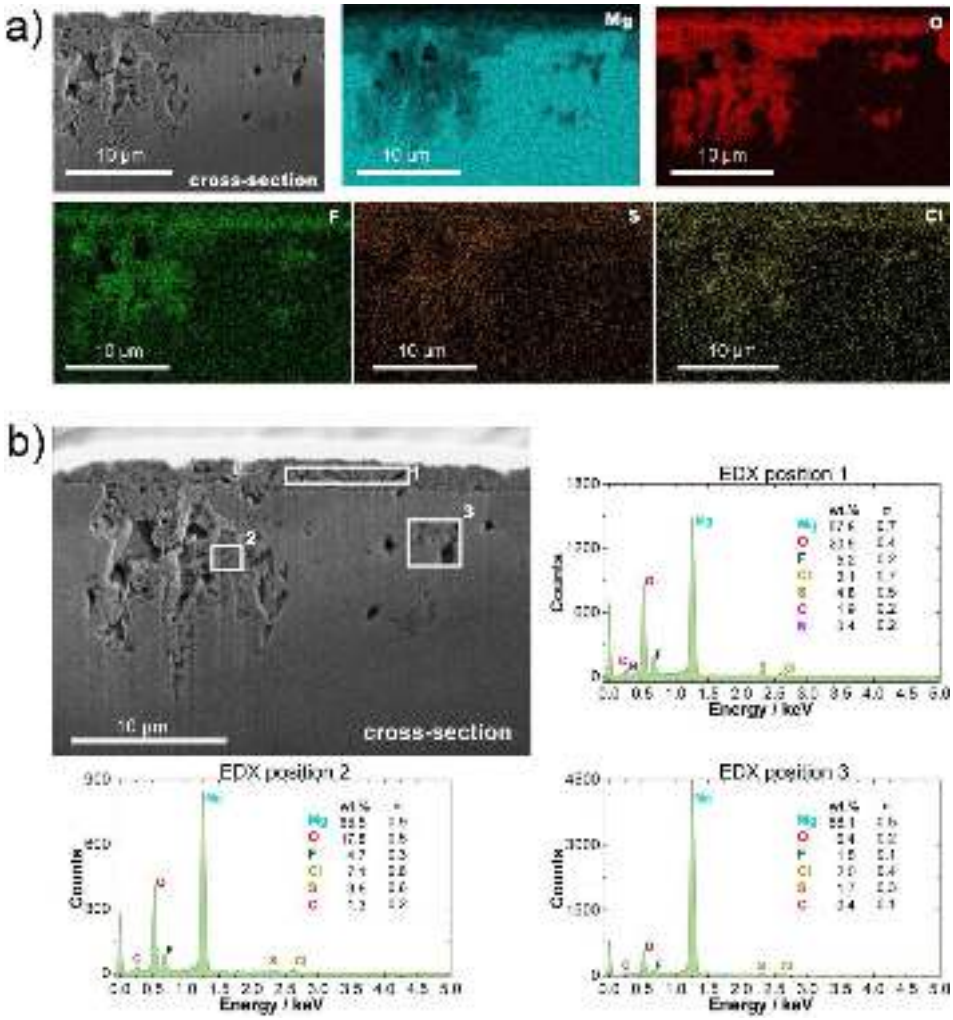

Figure S9. a)*.EDX cross-section mapping for cycled Mg electrode with catholyte and* ***b)*** *quantitative EDX spectra of selected areas*

XPS of cycled Mg electrode surfaces with different electolytes

Table S2. Atomic elemental composition for Mg electrode in concentrated TFSI electrolyte

Ar^+ ion sputter time / s	O At.%	F At.%	Mg At.%	C At.%	S At.%	Cl At.%
0	30.6	19.0	5.7	32.9	6.4	/
30	33.9	13.3	41.0	9.4	0.4	/
60	33.5	11.4	44.3	8.1	1.1	/
150	33.5	9.2	49.4	5.8	1.0	/
330	34.1	7.1	53.2	0.04	0.5	/

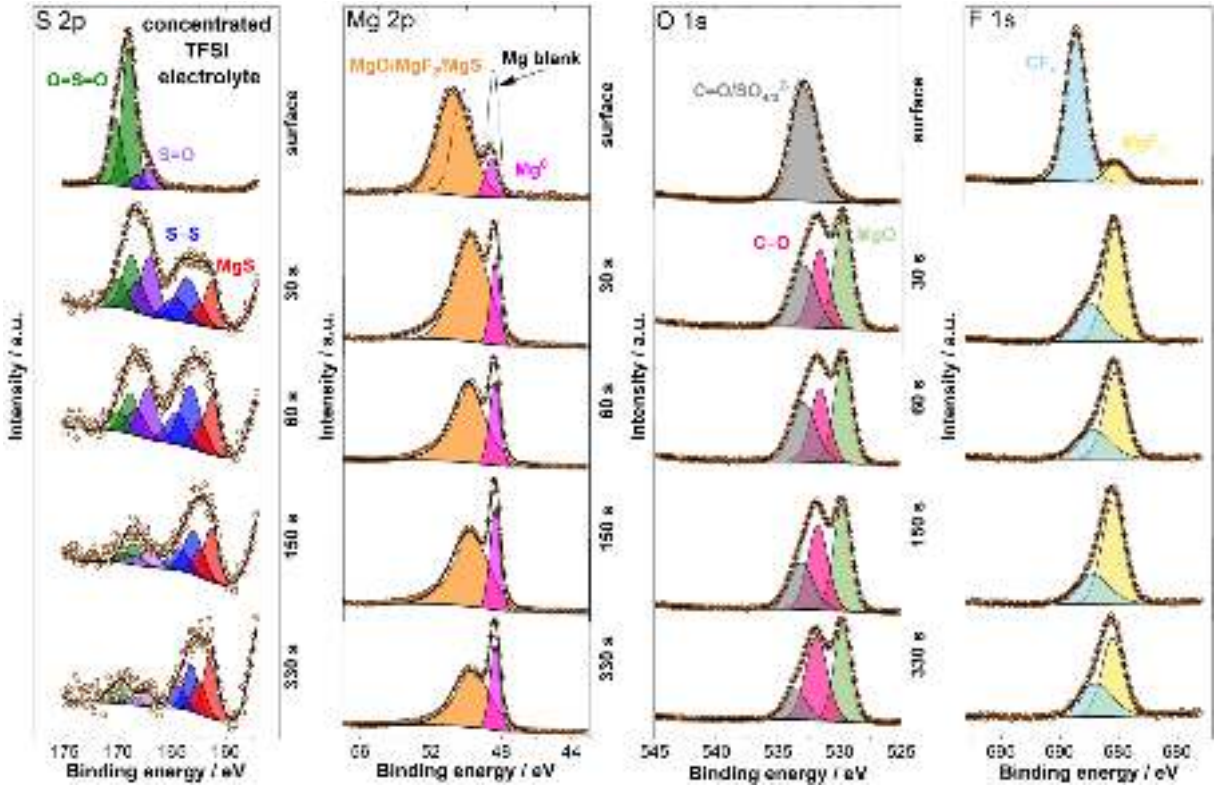

Figure S10. *XPS spectra before and after 30 s, 60 s, 150 s and 330 s of Ar^+ ion sputtering for cycled Mg electrode in concentrated TFSI electrolyte.*

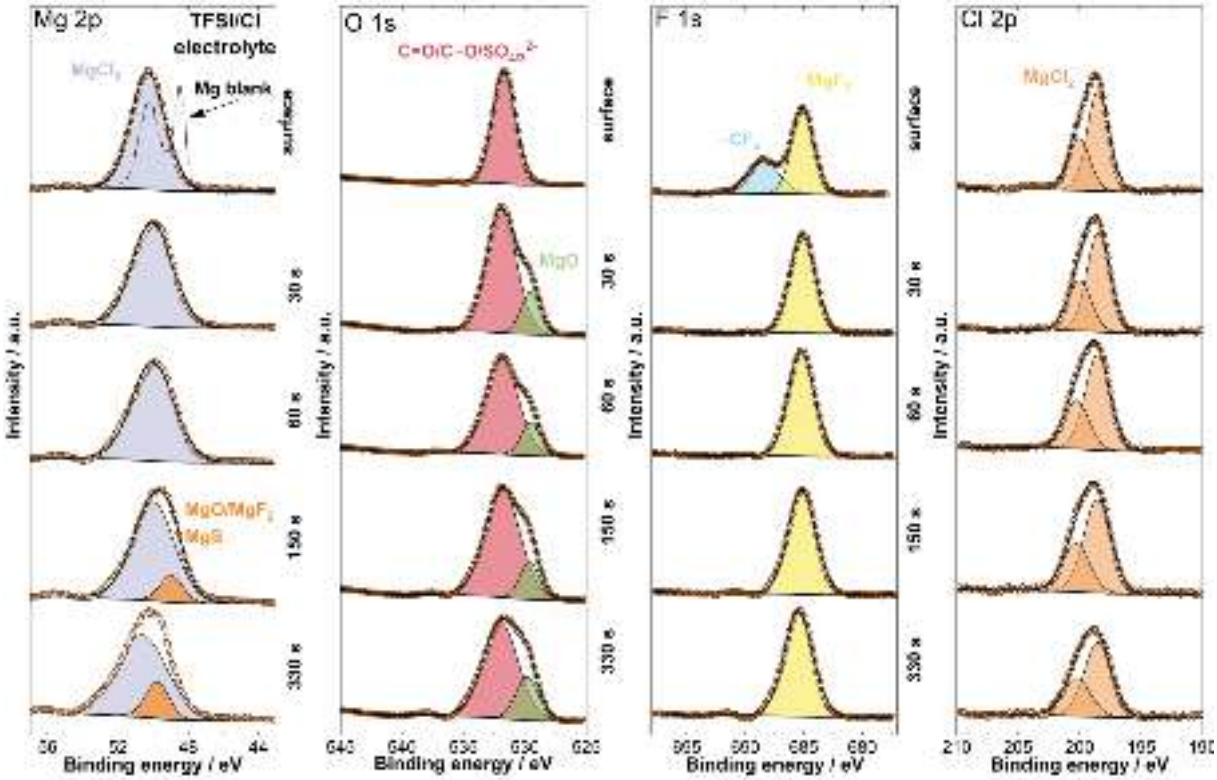

Figure S11. *XPS spectra before and after 30 s, 60 s, 150 s and 330 s of Ar^+ ion sputtering for cycled Mg electrode in TFSI/Cl electrolyte.*

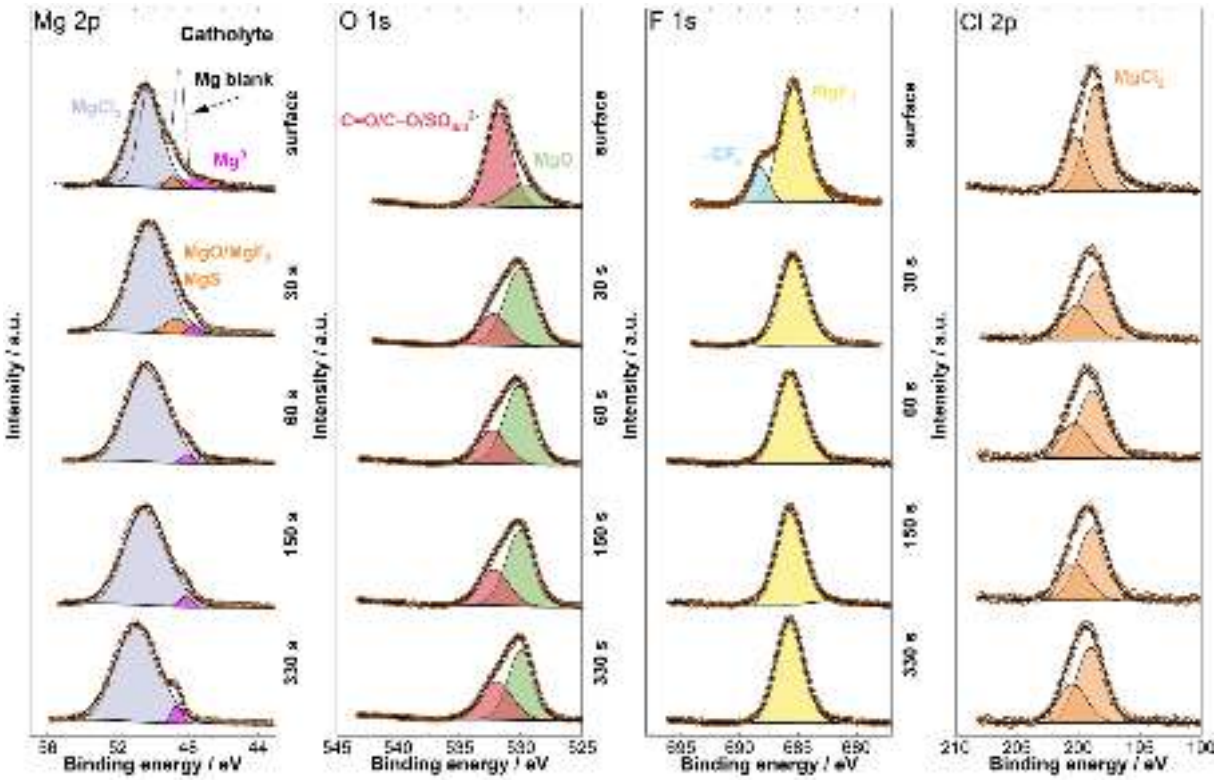

Figure S12: *XPS spectra before and after 30 s, 60 s, 150 s and 330 s of Ar^+ ion sputtering for cycled Mg electrode catholyte.*

Table S3. S 2p binding energies obtained after the fitting procedures.

		Concentrated TFSI electrolyte					TFSI/Cl electrolyte					catholyte				
		0s	**30s**	**60s**	**150s**	**330s**	**0s**	**30s**	**60s**	**150s**	**330s**	**0s**	**30s**	**60s**	**150s**	**330s**
S2p	**MgS**		161.3	161.3	161.3	161.4		161.5	161.5	161.6	161.5	161.6	161.5	161.5	161.5	161.5
	S–S		163.6	163.3	163.1	163.2	163.1	163.5	163.6	163.8	164.1	164.0	164.0	164.0	163.7	163.3
	S=O	167.2	167.1	167.3	167.1	167.4	168.5	167.6	167.7	167.1	167.2	166.7	166.7	167.4	167.5	167.9
	O=S=O	169.2	168.9	168.9	168.8	169.1	169.6	169.5	169.7	169.4	169.4	168.2	168.3			

Table S4. Sulfur species atomic composition on cycled Mg electrode in concentrated TFSI electrolyte.

	Surface	**30 s**	**60 s**	**150 s**	**330 s**
Total S at.%	6.4	0.4	1.1	1	0.5
O=S=O at.%	5.4	0.1	0.2	0.1	0.1
S=O at.%	0.9	0.1	0.3	0.1	0.1
S–S at.%	0	0.1	0.4	0.4	0.2
MgS at.%	0	0.1	0.3	0.3	0.2

Table S5. Sulfur species atomic composition on cycled Mg electrode in TFSI/Cl electrolyte

	Surface	**30 s**	**60 s**	**150 s**	**330 s**
Total S at.%	1.9	1.5	1.1	0.10	0.10
O=S=O at.%	0.4	0.3	0.2	0.04	0.03
S=O at.%	1.4	0.7	0.6	0.04	0.02
S–S at.%	0.2	0.2	0.1	0.01	0.01
MgS at.%	0	0.3	0.2	0.04	0.03

Table S6. Sulfur species atomic composition on cycled Mg electrode in catholyte.

	Surface	**30 s**	**60 s**	**150 s**	**330 s**
Total S at.%	2.7	2.2	2.5	2.4	2.6
O=S=O at.%	0.9	0.2	0.0	0.0	0.0
S=O at.%	0.7	0.3	0.5	0.3	0.2
S–S at.%	0.2	0.3	0.2	0.2	0.4
MgS at.%	1.0	1.5	1.9	1.9	2.1

References

[1] M. Keddam, O.R. Mottos, H. Takenouti, Reaction Model for Iron Dissolution Studied by Electrode Impedance: I . Experimental Results and Reaction Model, J. Electrochem. Soc. 128 (1981) 257–266. https://doi.org/10.1149/1.2127401.

[2] M. Keddam, J. -F. Lizee, C. Pallotta, H. Takenouti, Electrochemical Behavior of Passive Iron in Acid Medium: I . Impedance Approach, J. Electrochem. Soc. 131 (1984) 2016–2024. https://doi.org/10.1149/1.2116010.

[3] R. Antaño-Lopez, M. Keddam, H. Takenouti, A new experimental approach to the time-constants of electrochemical impedance: frequency response of the double layer capacitance, Electrochim. Acta. 46 (2001) 3611–3617. https://doi.org/10.1016/S0013-4686(01)00640-5.

[4] D. Strmčnik, M. Gaberšček, B. Pihlar, D. Kočar, J. Jamnik, Copper Dissolution in Ammonia Solutions: Identification of the Mechanism at Low Overpotentials, J. Electrochem. Soc. 156 (2009) C222. https://doi.org/10.1149/1.3123289.